Scaling and memory in the return intervals of energy dissipation rate in three-dimensional fully developed turbulence

Chuang Liu (刘闯),[1,2] Zhi-Qiang Jiang (蒋志强),[1,3] Fei Ren (任飞),[1,2,4] and Wei-Xing Zhou (周炜星)[1,2,3,4,5,*]

[1]*School of Business, East China University of Science and Technology, Shanghai 200237, China*

[2]*Engineering Research Center of Process Systems Engineering (Ministry of Education), East China University of Science and Technology, Shanghai 200237, China*

[3]*School of Science, East China University of Science and Technology, Shanghai 200237, China*

[4]*Research Center for Econophysics, East China University of Science and Technology, Shanghai 200237, China*

[5]*Research Center on Fictitious Economics & Data Science, Chinese Academy of Sciences, Beijing 100080, China*

(Received 9 January 2009; revised manuscript received 25 June 2009; published 5 October 2009)

We study the statistical properties of return intervals r between successive energy dissipation rates above a certain threshold Q in three-dimensional fully developed turbulence. We find that the distribution function $P_Q(r)$ scales with the mean return interval R_Q as $P_Q(r)=R_Q^{-1}f(r/R_Q)$ for $R_Q \in [50,500]$, where the scaling function $f(x)$ has two power-law regimes. The scaling behavior is statistically validated by the Cramér–von Mises criterion. The return intervals are short-term and long-term correlated and possess multifractal nature. The Hurst index of the return intervals decays exponentially against R_Q, predicting that rare extreme events with $R_Q \to \infty$ are also long-term correlated with the Hurst index $H_\infty=0.639$. These phenomenological findings have potential applications in risk assessment of extreme events at very large R_Q.

DOI: 10.1103/PhysRevE.80.046304 PACS number(s): 47.27.Jv, 05.45.Tp, 47.53.+n, 89.75.Da

I. INTRODUCTION

Extreme events are ubiquitous in nature and society and understanding their dynamics is of crucial importance [1,2]. However, extreme events are usually rare, which makes it difficult to investigate their occurrence properties. Recently, there is an increasing interest in the study of return intervals or reoccurrence times r between successive events above (or below) some threshold Q, aiming at unveiling the laws governing the occurrence of extreme events by studying the statistics of the return intervals for increasing threshold Q.

Recent studies show that the long-term correlation structure has essential influence on the statistics of return intervals [3]. For long-term power-law correlated monofractal records with exponent γ, numerical analysis illustrates that the distribution density function of the return intervals follows a stretched exponential $P_Q(r) \sim \exp[-b(r/R_Q)^\gamma]$ with the same exponent γ and the return intervals are also long-term correlated, again with the same exponent γ, where R_Q is the mean return interval associated with threshold Q [4–6]. Uncorrelated records with $\gamma=1$ is a special case, whose return intervals are exponentially distributed. When $0<\gamma\leq 1$, theoretical analysis with certain approximation shows that the distribution of return interval is Weibull: $P_Q(r) \sim r^{\gamma-1} \times \exp(-cr^\gamma)$ [7,8]. This seems consistent with recent numerical results [9].

For multifractal records in the presence or absence of linear correlations, extensive simulations based on the multiplicative random cascade (MRC) model [10] and the multifractal random walk (MRW) model [11] unveil that the return intervals have a power-law decay in the distribution and are long-term correlated governed by power laws whose exponents depend explicitly on the threshold Q, and the conditional return intervals increase as a power-law function of the previous return interval [12–14]. These results are of particular interest since a variety of time series exhibit multifractal nature. For instance, the returns of common stocks can be well modeled by the multifractal random walk [15,16], and the statistics of the associated return intervals are found to comply with the numerical prediction [12,14], which can be used to significantly improve risk estimation [12].

Another important issue of multifractal records concerns the possible scaling behavior of the return interval distributions $P_Q(r)$ over different thresholds Q. Numerical simulations of MRC and MRW time series find no evidence of such scaling [12–14]. However, empirical return interval analysis of financial volatility gives miscellaneous results. Several studies reported that there is a scaling law in the return interval distributions [17–21], while others argued that the cumulative distributions of return intervals had systematic deviations from scaling and showed multiscaling behaviors [22–25].

II. DATA

In this work, we perform return interval analysis of the energy dissipation rate in three-dimensional fully developed turbulence based on a high-Reynolds turbulence data set collected at the S1 ONERA wind tunnel by the Grenoble group from LEGI [26]. The size of the velocity time series $\{v_i: i=1,2,\ldots,N\}$ is about 1.73×10^7. Using Taylor's frozen flow hypothesis which replaces a spatial variation of the fluid velocity by a temporal variation measured at a fixed location, the rate of kinetic energy dissipation at position i is $\epsilon_i \sim [(v_{i+1}-v_i)/\delta_\ell]^2$, where $\delta_\ell=0.72$ mm is the resolution (translated in spatial scale) of the measurements. The energy dissipation rate time series exhibit multifractal nature [27] and its Hurst index is $H=1-\gamma/2=0.81$. Contrary to previous studies on simulated signals and real signals other than tur-

*wxzhou@ecust.edu.cn

bulence signals, we find that the return interval distributions show two power-law regimes and collapse onto a single curve for different thresholds Q. The scaling phenomenon is also observed for conditional interval distributions.

The mean velocity of the flow is approximately $\langle v\rangle = 20$ m/s (compressive effects are thus negligible). The root-mean-square velocity fluctuations is $v_{\rm rms}=1.7$ m/s, leading to a turbulence intensity equal to $I=v_{\rm rms}/\langle v\rangle=0.0826$. This is sufficiently small to use Taylor's frozen flow hypothesis. The integral scale is approximately 4 m but is difficult to estimate precisely as the turbulent flow is neither isotropic nor homogeneous at these large scales.

The Kolmogorov microscale η is given by [28] $\eta = [\nu^2\langle v\rangle^2/15\langle(\partial v/\partial t)^2\rangle]^{1/4}=0.195$ mm, where $\nu=1.5\times10^{-5}$ m^2 s^{-1} is the kinematic viscosity of air. $\partial v/\partial t$ is evaluated by its discrete approximation with a time step increment $\partial t=3.5466\times10^{-5}$ s corresponding to the spatial resolution δ_ℓ divided by $\langle v\rangle$, which is used to transform the data from time to space applying Taylor's frozen flow hypothesis. The Taylor scale is given by [28] $\lambda=\langle v\rangle v_{\rm rms}/\langle(\partial v/\partial t)^2\rangle^{1/2}=16.6$ mm. The Taylor scale is thus about 85 times the Kolmogorov scale. The Taylor-scale Reynolds number is $\mathrm{Re}_\lambda=\lambda v_{\rm rms}/\nu=2000$. This number is actually not constant along the whole data set and fluctuates by about 20%.

We have checked that the standard scaling laws previously reported in the literature are recovered with this time series. In particular, we have verified the validity of the power-law scaling $E(k)\sim k^{-\beta}$ with an exponent β very close to 5/3 over a range more than two decades, similar to Fig. 5.4 of Ref. [29] provided by Gagne and Marchand on a similar data set from the same experimental group. The inertial range can be regarded as the length scales between the Taylor scale λ and the integral scale L, which leads to $\lambda/\delta_\ell \ll \ell/\delta_\ell \ll L/\delta_\ell$ or equivalently $23 \ll r \ll 5000$.

III. DISTRIBUTION AND RISK

A. Unconditional PDF

We have calculated the return interval time series r_i for different thresholds Q, which can be mapped nonlinearly to the mean return intervals R_Q. Logarithmic binning is adopted to construct the distribution density functions $P_Q(r)$. In order to ensure that the bins cover the whole r axis, we use the following procedure. First, the interval $[1,\max(r_i)]$ is partitioned logarithmically into $n-1$ subintervals whose edges are $x_1<x_2<\cdots<x_n$. Then we obtain the sequence $y_i=[x_i]$, where $[x_i]$ is a round function of x_i. We discard duplicate integers in the y_i sequence and obtain a new sequence w_j. The edge sequence of the bins are determined by $\{e_i\}=\{0.5,\{w_i+0.5\}\}$. For each bin $(e_i,e_{i+1}]$, the empirical density function can be calculated by

$$P_Q(r_i)=\frac{\#(e_i<r<e_{i+1})}{\#(r>0)}\frac{1}{e_{i+1}-e_i}, \tag{1}$$

where $r_i=(e_i+e_{i+1})/2$ and $\#(\ )$ denotes the number of return intervals that satisfies the condition in the parenthesis.

The empirical distribution of the return intervals is depicted in Fig. 1 for $R_Q=50$, 150, and 500. We find that the three distributions collapse onto a single curve except for $r=1$, in remarkable contrast to the simulation results for MRC and MRW time series. The absence of scaling for $r=1$ is probably due to a discreteness effect. Two power-law regimes are observed

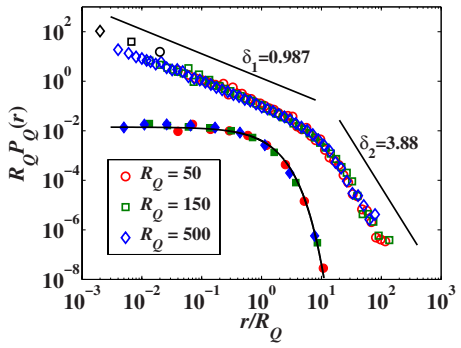

FIG. 1. (Color online) Log-log plot of the scaled distribution $R_Q P_Q(r)$ as a function of r/R_Q for three different values of R_Q. The straight lines are the best fits to power laws. The power-law exponents are $\delta_1=0.987$ and $\delta_2=3.88$. For the shuffled data, the $R_Q P_Q(r)$ curves collapse to a same exponential curve, as expected.

$$R_Q P_Q(r)\sim\begin{cases}A_1(r/R_Q)^{-\delta_1} & \text{if } 1<r<r_c\\ A_2(r/R_Q)^{-\delta_2} & \text{if } r>r_c,\end{cases} \tag{2}$$

where $A_1=0.107$, $A_2=33.4$, $\delta_1=0.987$, and $\delta_2=3.88$. For the shuffled data, the $R_Q P_Q(r)$ curves collapse to a single exponential curve.

In order to confirm quantitatively the existence of scaling behavior, we perform statistical test based on the Cramér–von Mises criterion. The Cramér–von Mises criterion was used for judging the goodness-of-fit of the probability distribution compared to a given distribution [30,31], which is given by

$$C_M^2=n\int_{-\infty}^{+\infty}[F(v)-F^*(v)]^2dF(v), \tag{3}$$

where F^* is the empirical cumulative distribution function, and F is the corresponding theoretical distribution. This approach can be easily extended for two-sample cases where $F(v)$ and $F^*(v)$ are the empirical cumulative distributions of the two samples. If the statistic C_M^2 is less than the critical value at a given significance level, we can say that the two samples are drawn from a same distribution. We perform the test on each pair of the three samples with $R_Q=50,150,500$ by excluding $r=1$. For the $R_Q=50$ and $R_Q=150$ samples, $C_M^2=0.173$ and the p value is 0.327. For the $R_Q=50$ and $R_Q=500$ samples, $C_M^2=0.359$ and the p value is 0.093. For the $R_Q=150$ and $R_Q=500$ samples, $C_M^2=0.106$ and the p value is 0.553. It is evident that all the three pairs of the rescaled distributions are identical at the significance level of 5% where the critical value is 0.461.

The above test shows that there is a scaling behavior in Fig. 1 for $R_Q\in[50,500]$. When $R_Q\gg500$, the distribution is unstable and lack of statistics. When $R_Q<50$, the scaling behavior disappears. For instance, we find that the return interval distribution for $R_Q=10$ is very different from those

shown in Fig. 1. However, the behavior of return intervals for small R_Q is of less important since we are interested in large (or extreme) velocity fluctuations. The scaling behavior for large R_Q values has practical applications in risk assessment that we will discuss later in this work.

We have also performed the Cramér–von Mises test to check if the tails decay in a power law. We find that the Cramér–von Mises statistic $C_M^2=0.710$ and the p value is 0.013 for $R_Q=50$, $C_M^2=0.571$ and $p=0.027$ for $R_Q=150$, and $C_M^2=0.072$ and $p=0.738$ for $R_Q=500$, respectively. Hence, we can not reject the hypothesis that the tails follow power-law distributions at the significance level of 1%. Using the data with $r>r_cR_Q$, the method of Clauset, Shalizi and Newman gives that the power-law exponent is $\delta_2=3.93$ for $R_Q=50$, $\delta_2=3.80$ for $R_Q=150$, and $\delta_2=4.02$ for $R_Q=500$ [32]. These values are consistent with $\delta_2=3.88$ shown in Fig. 1.

An important question asks whether the observations (such as the first scaling exponent which is compatible to 1.0 and the crossover of two regimes in the distributions) are related to the important scales in turbulence. Indeed, large return intervals correspond to large scales and small return intervals correspond to the dissipation region. As we have shown in Sec. II, the inertial range is $23 \ll r \ll 5000$. The average return intervals $R_Q \in [50,500]$ show that the crossover point is well within the inertial region, which is independent of the dissipation region and the integral injection scale. Indeed, the crossover r_cR_Q is not a constant but depends on R_Q, which is thus impossible to be relevant to any turbulence scales. However, a physical explanation of this crossover phenomenon is lack.

B. Risk estimation

In risk estimation, a quantity of great interest is the probability $W_Q(\Delta t,t)$ that an extreme event occurs after a short time $\Delta t \ll t$ from now on, conditioned that the time elapsed t after the occurrence of the previous extreme event [12],

$$W_Q(\Delta t|t) = \frac{\int_t^{t+\Delta t} P_Q(t)dt}{\int_t^{\infty} P_Q(t)dt}. \tag{4}$$

When $t>r_c$, simple algebraic manipulation leads to

$$W_Q(\Delta t|t) \simeq (\delta_2 - 1)\Delta t/t. \tag{5}$$

The probability $W_Q(\Delta t|t)$ is found to be proportional to Δt and inversely proportional to t. An intriguing feature is that $W_Q(\Delta t|t)$ is independent of the threshold Q, which is a direct consequence of the scaling behavior of $P_Q(r)$ shown in Fig. 1. When $t<r_c$, we obtain that

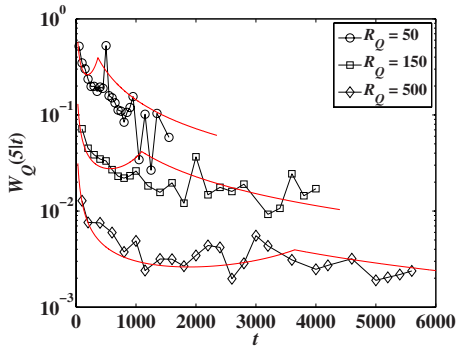

FIG. 2. (Color online) Comparison of $W_Q(\Delta t=5|t)$ estimated empirically with that obtained from Eqs. (5) and (6) for different R_Q. The curves for $R_Q=150$ and $R_Q=50$ have been shifted vertically by factors of 0.5 and 1 for clarity.

$$W_Q(\Delta t|t) \approx \frac{(\delta_1-1)\left(\frac{t}{R_Q}\right)^{-\delta_1}\frac{\Delta t}{R_Q}}{\left(\frac{t}{R_Q}\right)^{1-\delta_1} + \frac{A_2}{A_1}\frac{\delta_1-1}{\delta_2-1}\left(\frac{r_c}{R_Q}\right)^{1-\delta_2} - \left(\frac{r_c}{R_Q}\right)^{1-\delta_1}}$$
$$\approx \frac{(\delta_1-1)\left(\frac{t}{R_Q}\right)^{-\delta_1}\frac{\Delta t}{R_Q}}{\left(\frac{t}{R_Q}\right)^{1-\delta_1} - 1.0308}. \tag{6}$$

We find that $W_Q(\Delta t|t)$ is proportional to Δt. However, $W_Q(\Delta t|t)$ also depends on R_Q. Since $W_Q(\Delta t|t)$ should be continuous at $t=r_c$, combining Eqs. (5) and (6), we have

$$r_c/R_Q = (A_2/A_1)^{1/(\delta_2-\delta_1)} = 7.28. \tag{7}$$

Figure 2 confirms numerically the validity of Eqs. (5) and (6) by comparing the theoretical curves with the empirical curves obtained from the definition (4).

IV. MEMORY EFFECTS

A. Short memory

In order to test the memory effects of the return intervals, we first investigate the conditional PDF $P_Q(r|r_0)$, which is the distribution of return intervals immediately after r_0. To gain better statistics, we study $P_Q(r|r_0)$ for a range of r_0 rather than individual r_0 values. For each threshold Q or R_Q, the return intervals sequence are sorted in an increasing order and then divided into eight groups $G_1,\ldots,G_8$ with approximately equal size. An empirical conditional distribution is determined for each r_0 group. Figure 3 shows $P_Q(r|r_0)$ for $r_0 \in G_1$ and $r_0 \in G_8$. For each group, the three distributions collapse onto a single curve, indicating evident scaling behavior. The figure shows that the probability of finding small (large) r in G_1 is enhanced (decreased) compared with G_8. This discrepancy in the two groups of distributions unveils the memory effect that large (small) return intervals tend to follow large (small) return intervals. This is true since the distributions associated with different G_i should not exhibit significant discrepancy if there is no memory in the return intervals [17].

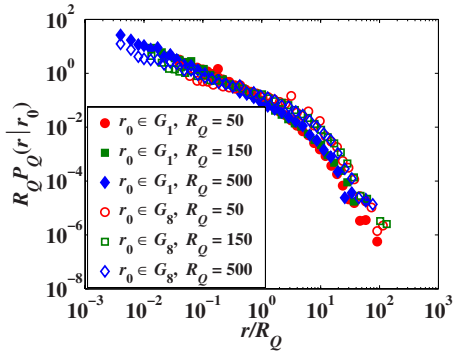

FIG. 3. (Color online) Scaling and memory in the conditional distributions. The scaled conditional distribution $R_Q P_Q(r|r_0)$ is plotted as a function of r/R_Q with r_0 in G_1 and G_8 for three different values of R_Q.

The memory effect in the conditional distribution $P_Q(r|r_0)$ can also be illustrated by the mean conditional return interval $\langle r|r_0\rangle$. If there is no memory in the return intervals, $\langle r|r_0\rangle$ does not depend on r_0 and is equal to R_Q. Figure 4 plots the mean conditional return interval $\langle r|r_0\rangle$ as a function of r_0 for R_Q=50, 150, and 500. It is shown that $\langle r|r_0\rangle$ is a power-law function of r_0 when r_0 is larger than certain value and the power-law exponent decreases with R_Q, which is consistent with many simulational and empirical studies. Also shown in Fig. 4 is the mean conditional return interval of the shuffled energy dissipation rate, which does not depend on r_0.

B. Long-term memory

We now study the long-term correlation in the return intervals using the multifractal detrended fluctuation analysis (MFDFA) [33]. The MFDFA considers the cumulative time series $R_i=\Sigma_{i=1}^{m}(r_i-\langle r\rangle)$, which is partitioned into N_s disjoint boxes with the same size s. In each box k, the local trend is removed from the subseries by a polynomial function and the local rms fluctuation $f_k(s)$ is determined. The overall detrended fluctuation can be calculated by

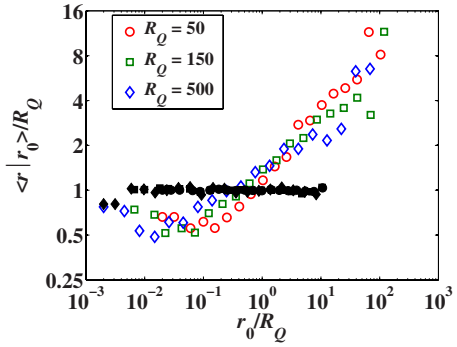

FIG. 4. (Color online) Scaled mean conditional return interval $\langle r|r_0\rangle/R_Q$ versus r_0/R_Q of return interval sequence in turbulence for various R_Q. The filled symbols represent the results for the shuffled records without memory.

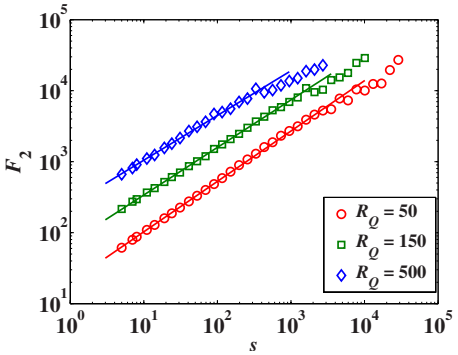

FIG. 5. (Color online) Detrended fluctuation analysis of the return interval time series for different R_Q.

$$F_q(s) = \left\{ \frac{1}{N_s} \sum_{k=1}^{N_s} [f_k(s)]^q \right\}^{1/q}. \tag{8}$$

By varying the value of s, one can expect the detrended fluctuation function $F_q(s)$ scales with the size s,

$$F_q(s) \sim s^{h(q)}, \tag{9}$$

where $h(q)$ is the generalized Hurst index. The return interval series possesses multifractal nature if and only if $h(q)$ is a nonlinear function of q. When q=2, $h(2)$ is nothing but the Hurst index H and the MFDFA reduces to the DFA. The Hurst index H is related to the autocorrelation exponent γ by $\gamma=2-2H$.

We first investigate the linear long-term correlation property of the return intervals using DFA. The dependence of the fluctuation function F_2 is drawn in Fig. 5 against s for R_Q =50, 150, and 500. In all cases, we find nice power-law relation and the scaling range decreases with the increase of R_Q.

Figure 6 illustrates the dependence of H with respect to R_Q. We find that the relation between H and R_Q can be fitted by an exponential decay,

$$H = H_\infty + be^{-R_Q/R_c} = 0.639 + 0.158e^{-R_Q/69.9}, \tag{10}$$

where R_c=69.9 is the characteristic scale. The inset of Fig. 6 plots $H=H_\infty$ against R_Q in log-linear coordinates. The nice linearity of the data points confirms the validity of Eq. (10). For extreme events with very large Q, R_Q tends to infinity,

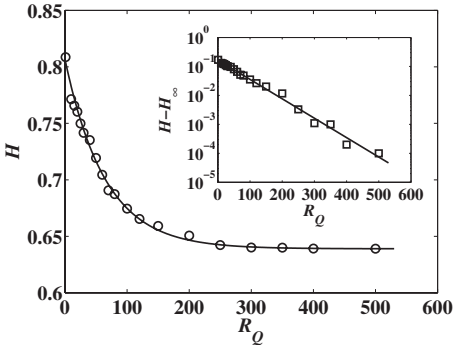

FIG. 6. Dependence of H with respect to R_Q. The inset shows the exponential decay of the Hurst index $H-H_\infty$ against R_Q.

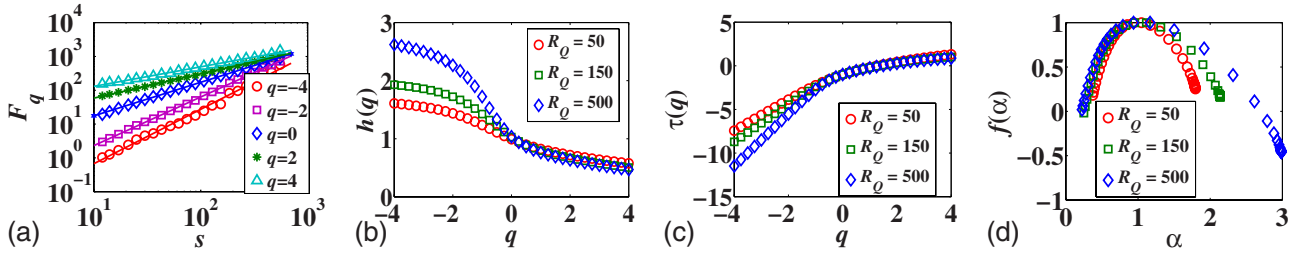

FIG. 7. (Color online) Multifractal detrended fluctuation analysis of the return interval time series for different R_Q. (a) MFDFA fluctuation function for different q when R_Q=50. (b) Generalized Hurst indexes $h(q)$. (c) Mass scaling exponents $\tau(q)$. (d) Multifractal singularity spectra $f(\alpha)$.

and the Hurst index can be predicted as $H=H_\infty=0.639$. This implies that the return intervals of those extreme events also exhibit long-term memory.

Previous empirical analysis has unveiled that the long-term correlation in the return intervals is related to the long-term correlation in the original data and the return intervals become uncorrelated if we shuffle the original data [17]. The turbulent signal investigated in this work has a strong correlation, which might cause the correlation in its return intervals. For extreme events at very large R_Q, it is hard to check if the return intervals are correlated or not due to the lack of statistics. Our phenomenological finding Eq. (10) provides an important conjecture that the return intervals are also correlated. This provides a potential application in the anticipation of return intervals between extreme events. We stress that the determination of H_∞ is completely numerical, and we do not have a theory to derive the expression (10). No such a derivation has been given even for fractional Brownian motions or multifractal signals.

C. Multifractality

We also apply the MFDFA to investigate the multifractal nature of the return intervals. Figure 7(a) shows the power-law dependence of the overall fluctuation $F_q(s)$ on the scale s for R_Q=50. When R_Q increases, the $F_q(s)$ function becomes more noisy, especially for negative q. The slopes of the straight lines are the linear least-squares estimates of the generalized Hurst indexes $h(q)$, which are drawn in Fig. 7(b). The mass scaling exponent function $\tau(q)=qh(q)-1$ and the multifractal spectrum $f(\alpha)$ calculated according to the Legendre transform of $\tau(q)$ are illustrated, respectively, in Figs. 7(c) and 7(d). The sound nonlinearity in $h(q)$ and $\tau(q)$ is a hallmark of multifractality in the return intervals, whose singularity strength increases with R_Q.

V. SUMMARY

In summary, we have studied the statistical properties of return intervals of the energy dissipation rate in three-dimensional fully developed turbulence. The interval distribution is found to exhibit scaling behavior across different R_Q and two power-law regimes, except for intervals $r=1$. We found that the conditional interval distributions also collapse onto a single curve for same r_0, but deviate for different r_0, and the mean conditional interval increases as a power law of r_0, which indicates the presence of short memory in the return intervals. The long-term memory and the multifractal nature in the return intervals are confirmed by the DFA and MFDFA. The Hurst index of the return intervals decays exponentially against R_Q, which allows us to predict the asymptotic Hurst index of return intervals between rare extreme events as $H_\infty=0.639$.

The multiplicative random cascade model [10] (and the same happens for the multifractal random walk model [11]) has been developed in order to mimic the multifractality of a turbulent signal. These models are very successful in reproducing many "stylized facts" of turbulence. Extensive simulations based on the MRC model and the MRW model unveiled that the return intervals have a power-law decay in the distribution without any evidence of a scaling behavior and are long-term correlated governed by power laws whose exponents depend explicitly on the threshold Q (or R_Q) [12–14]. Our results signify discrepancy with the numerical results using MRC and MRW models, implying that the energy dissipation process can not be modeled using these models. In other words, these two models are not able to capture the behaviors of extreme events.

ACKNOWLEDGMENTS

This work was partially supported by the National Basic Research Program of China (Grant No. 2004CB217703), the Program for Changjiang Scholars and Innovative Research Team in University (Grant No. IRT0620), the National Natural Science Foundation (Grant No. 10905023), the Natural Science Foundation of Zhejiang Provence of China (Grant No. Z6090130, and the Program for New Century Excellent Talents in University (Grant No. NCET-07-0288).

[1] *The Science of Disasters*, edited by A. Bunde, J. Kropp, and H.-J. Schellnhuber (Springer, Berlin, 2005).
[2] K. Y. Kondratyev, C. A. Varotsos, and V. F. Krapivin, *Natural Disasters as Interactive Components of Global Ecodynamics* (Springer, Berlin, 2006).
[3] M. I. Bogachev, J. F. Eichner, and A. Bunde, Pure Appl. Geophys. **165**, 1195 (2008).
[4] A. Bunde, J. F. Eichner, S. Havlin, and J. W. Kantelhardt, Physica A **330**, 1 (2003).
[5] A. Bunde, J. F. Eichner, J. W. Kantelhardt, and S. Havlin, Phys. Rev. Lett. **94**, 048701 (2005).
[6] E. G. Altmann and H. Kantz, Phys. Rev. E **71**, 056106 (2005).
[7] P. Olla, Phys. Rev. E **76**, 011122 (2007).
[8] M. S. Santhanam and H. Kantz, Phys. Rev. E **78**, 051113 (2008).
[9] J. F. Eichner, J. W. Kantelhardt, A. Bunde, and S. Havlin, Phys. Rev. E **75**, 011128 (2007).
[10] C. Meneveau and K. R. Sreenivasan, Phys. Rev. Lett. **59**, 1424 (1987).
[11] E. Bacry, J. Delour, and J.-F. Muzy, Phys. Rev. E **64**, 026103 (2001).
[12] M. I. Bogachev, J. F. Eichner, and A. Bunde, Phys. Rev. Lett. **99**, 240601 (2007).
[13] M. I. Bogachev, J. F. Eichner, and A. Bunde, Eur. Phys. J. Spec. Top. **161**, 181 (2008).
[14] M. I. Bogachev and A. Bunde, Phys. Rev. E **78**, 036114 (2008).
[15] J.-F. Muzy, J. Delour, and E. Bacry, Eur. Phys. J. B **17**, 537 (2000).
[16] E. Bacry, J. Delour, and J.-F. Muzy, Physica A **299**, 84 (2001).
[17] K. Yamasaki, L. Muchnik, S. Havlin, A. Bunde, and H. E. Stanley, Proc. Natl. Acad. Sci. U.S.A. **102**, 9424 (2005).
[18] F.-Z. Wang, K. Yamasaki, S. Havlin, and H. E. Stanley, Phys. Rev. E **73**, 026117 (2006).
[19] F. Wang, P. Weber, K. Yamasaki, S. Havlin, and H. E. Stanley, Eur. Phys. J. B **55**, 123 (2007).
[20] W.-S. Jung, F.-Z. Wang, S. Havlin, T. Kaizoji, H. T. Moon, and H. E. Stanley, Eur. Phys. J. B **62**, 113 (2008).
[21] T. Qiu, L. Guo, and G. Chen, Physica A **387**, 6812 (2008).
[22] F.-Z. Wang, K. Yamasaki, S. Havlin, and H. E. Stanley, Phys. Rev. E **77**, 016109 (2008).
[23] J. W. Lee, K. E. Lee, and P. A. Rikvold, J. Korean Phys. Soc. **48**, S123 (2006).
[24] F. Ren and W.-X. Zhou, EPL **84**, 68001 (2008).
[25] F. Ren, L. Guo, and W.-X. Zhou, Physica A **388**, 881 (2009).
[26] F. Anselmet, Y. Gagne, E. J. Hopfinger, and R. A. Antonia, J. Fluid Mech. **140**, 63 (1984).
[27] W.-X. Zhou and D. Sornette, Physica D **165**, 94 (2002).
[28] C. Meneveau and K. R. Sreenivasan, J. Fluid Mech. **224**, 429 (1991).
[29] U. Frisch, *Turbulence: The Legacy of A. N. Kolmogorov* (Cambridge University Press, Cambridge, England, 1996).
[30] D. A. Darling, Ann. Math. Stat. **28**, 823 (1957).
[31] T. W. Anderson, Ann. Math. Stat. **33**, 1148 (1962).
[32] A. Clauset, C. R. Shalizi, and M. E. J. Newman, SIAM Rev. (to be published).
[33] J. W. Kantelhardt, S. A. Zschiegner, E. Koscielny-Bunde, S. Havlin, A. Bunde, and H. E. Stanley, Physica A **316**, 87 (2002).